

✓ AD-A150 059

RESONANCE BETWEEN BETATRON AND SYNCHROTRON OSCILLATIONS
IN A FREE ELECTRON LASER: A 3-D NUMERICAL STUDY(U)
NAVAL RESEARCH LAB WASHINGTON DC C M TANG ET AL.

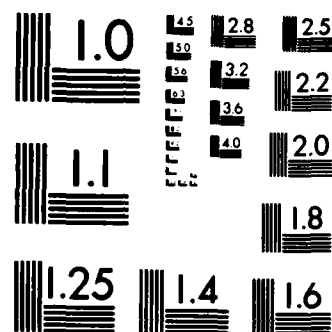
1/1

UNCLASSIFIED 30 JAN 85 NRL-MR-5499

F/G 20/5

NL





MICROCOPY RESOLUTION TEST CHART
NATIONAL BUREAU OF STANDARDS-1963-A

2

NRL Memorandum Report 5499

Resonance Between Betatron and Synchrotron Oscillations in a Free Electron Laser: A 3-D Numerical Study

C. M. TANG AND P. SPRANGLE

*Plasma Theory Branch
Plasma Physics Division*

January 30, 1985

This work was sponsored by the Defense Advanced Research Projects Agency
under Contract 3817.



NAVAL RESEARCH LABORATORY
Washington, D.C.

Approved for public release; distribution unlimited.

85 01 28 003

AD-A150 059

DTIC FILE COPY

DTIC
SELECTE
FEB 07 1985
D
E

114

AD-A150059

SECURITY CLASSIFICATION OF THIS PAGE

REPORT DOCUMENTATION PAGE				
1a REPORT SECURITY CLASSIFICATION UNCLASSIFIED		1b RESTRICTIVE MARKINGS		
2a SECURITY CLASSIFICATION AUTHORITY		3 DISTRIBUTION/AVAILABILITY OF REPORT Approved for public release; distribution unlimited.		
2b DECLASSIFICATION/DOWNGRADING SCHEDULE				
4 PERFORMING ORGANIZATION REPORT NUMBER(S) NRL Memorandum Report 5499		5 MONITORING ORGANIZATION REPORT NUMBER(S)		
6a NAME OF PERFORMING ORGANIZATION Naval Research Laboratory	6b OFFICE SYMBOL (If applicable) Code 4790	7a NAME OF MONITORING ORGANIZATION		
6c ADDRESS (City, State, and ZIP Code) Washington, DC 20375-5000		7b ADDRESS (City, State, and ZIP Code)		
8a NAME OF FUNDING/SPONSORING ORGANIZATION DARPA	8b OFFICE SYMBOL (If applicable)	9 PROCUREMENT INSTRUMENT IDENTIFICATION NUMBER		
8c ADDRESS (City, State, and ZIP Code) Arlington, VA 22209		10 SOURCE OF FUNDING NUMBERS		
		PROGRAM ELEMENT NO 62301E	PROJECT NO	TASK NO DN980-378
11 TITLE (Include Security Classification) Resonance Between Betatron and Synchrotron Oscillations in a Free Electron Laser: A 3-D Numerical Study				
12 PERSONAL AUTHOR(S) Tang, C.M. and Sprangle, P.				
13a TYPE OF REPORT Interim	13b TIME COVERED FROM TO	14 DATE OF REPORT (Year, Month, Day) 1985 January 30	15 PAGE COUNT 22	
16 SUPPLEMENTARY NOTATION This work was sponsored by the Defense Advanced Research Projects Agency under Contract 3817.				
17 COSATI CODES			18 SUBJECT TERMS (Continue on reverse if necessary and identify by block number)	
FIELD	GROUP	SUB-GROUP	Free electron laser, Betatron-synchrotron stability	
19 ABSTRACT (Continue on reverse if necessary and identify by block number)				
<p>We analyze the effect of betatron and synchrotron resonance on the gain process of the free electron laser (FEL) including betatron oscillations, finite beam emittance, self-consistent electron dynamics and a 3-D radiation field. Betatron oscillations force the electrons to be affected by an oscillatory radiation amplitude and phase in a Gaussian resonator radiation field. We show that not only can the radiation phase variation cause a resonance between approximately twice the betatron wavenumber and the synchrotron wavenumber, but the radiation amplitude variation in an FEL with efficiency enhancement schemes or just a tapered magnetic wiggler field amplitude B_w can also have a similar resonance effect. Numerical results for a 10 μm FEL are given. We find that for short wigglers, the effect of the betatron-synchrotron instability on the gain is negligible for Gaussian electron beams with radius less than 0.8 times the radiation beam spot size.</p>				
20 DISTRIBUTION/AVAILABILITY OF ABSTRACT <input checked="" type="checkbox"/> UNCLASSIFIED UNLIMITED <input type="checkbox"/> SAME AS RPT <input type="checkbox"/> DTIC USERS			21 ABSTRACT SECURITY CLASSIFICATION UNCLASSIFIED	
22a NAME OF RESPONSIBLE INDIVIDUAL C. M. Tang			22b TELEPHONE (Include Area Code) (202) 767-4148	22c OFFICE SYMBOL Code 4790

DD FORM 1473, 84 MAR

83 APR edition may be used until exhausted
All other editions are obsolete

SECURITY CLASSIFICATION OF THIS PAGE

CONTENTS

INTRODUCTION	1
BETATRON OSCILLATIONS IN A TAPERED WIGGLER	2
RADIATION FIELD	3
EQUATION OF PHASE	4
NUMERICAL EXAMPLES	7
ACKNOWLEDGMENT	9
REFERENCES	17

Accession For

NTIS GRA&I

DTIC TAB

Unannounced

Justification by Codes

and/or

and

A-1



**PREVIOUS PAGE
IS BLANK**

RESONANCE BETWEEN BETATRON AND SYNCHROTRON
OSCILLATIONS IN A FREE ELECTRON LASER:
A 3-D NUMERICAL STUDY

INTRODUCTION

In this paper, we will examine the resonance between the synchrotron wavenumber, i.e., the wavenumber associated with the bounce of the electron in the ponderomotive potential well, and twice the betatron wavenumber [1-5]. Betatron oscillations are caused by the transverse gradient of the wiggler [6-12]. There are a number of different sources for this resonance. In this paper, we will concentrate on the one caused by the Gaussian resonator radiation field first discussed by M. Rosenbluth in Ref. [1]. Another source of the resonance, described in detail in Ref [5], requires a tapered wiggler, but not a 3-D radiation field.

The wavefronts of the Gaussian TEM_{00} resonator radiation are spherical; the curvature is a function of radial and axial position. As electrons execute betatron oscillations in the transverse direction, the electrons are forced to sample varying wavefronts or a varying phase of the radiation field. The effect of that on the axial electron motion is equivalent to varying the radiation frequency, which results in a forced driving term in the modified pendulum equation with a wavenumber of $2k_\beta$, where k_β is the betatron wavenumber.

The amplitude of the TEM_{00} resonator radiation field has a Gaussian profile in the radial direction. As electrons execute betatron oscillations in the transverse direction, the electrons are forced to sample varying radiation amplitudes. In an FEL employing efficiency enhancement schemes, we find that the amplitude variation also contributes forced driving terms in the modified pendulum equation with wavenumber $2k_\beta$.

Betatron oscillations, in a wiggler whose magnetic field amplitude B_w is tapered, result in a spatially dependent axial electron momentum. The wavenumber of the axial momentum variation is also $2k_\beta$ (see Ref. [5]).

When $2k_\beta$ becomes approximately equal to the synchrotron wavenumber K_s , the phase of the electrons in the ponderomotive potential well can become unstable and electrons can become detrapped from the buckets. Since the principle of efficiency enhancement schemes [13-16] for the FEL is based on trapping the electrons, the loss of trapped electrons will

reduce the gain. In an FEL oscillator, a slightly reduced gain will increase the start-up time necessary to reach saturation. A significantly reduced gain per pass will also reduce the final saturated field amplitude as well.

In this paper, we will consider a realistic, arbitrarily tapered, linearly polarized, magnetic wiggler. The vector potential of the wiggler is expressed as

$$\mathbf{A}_w = A_w(z) \cosh(k_w(z)y) \cos\left(\int_0^z k_w(z') dz'\right) \hat{\mathbf{e}}_x, \quad (1)$$

where $A_w(z)$ and $k_w(z)$ are the slowly varying amplitude and wavenumber. We will consider an electron beam that is cold but possesses a finite emittance. The radiation field initially is taken to be a Gaussian TEM_{00} resonator mode with slowly varying amplitude and phase. Modeling of an exact 3-D radiation with higher order modes can be achieved with minor modifications.

BETATRON OSCILLATIONS IN A TAPERED WIGGLER

For a linearly polarized wiggler, there exists a constant of motion in the x-direction,

$$p_x - \frac{|e|\hbar}{c} A_x = p_{x0}, \quad (2)$$

where the constant p_{x0} is the canonical momentum. To obtain the betatron orbits, we will take $A_x \simeq \mathbf{A}_w \cdot \hat{\mathbf{e}}_x$, and $p_x \simeq \frac{|e|\hbar}{c} A_x + p_{x0}$. The particle motion in the x-direction can be obtained by integrating the momentum in the x-direction,

$$\tilde{x} \simeq \tilde{x} + \frac{\beta_{o\perp}(z)}{k_w(z)} \cosh(k_w(z)\tilde{y}) \sin\left(\int_0^z k_w(z') dz'\right), \quad (3)$$

where $\tilde{x} = x_o + \beta_{x0}z$, $\beta_{x0} = p_{x0}/\gamma m_o c$, \tilde{y} is a function of (y_o, p_{y0}, z) , x_o and y_o are the initial transverse coordinates, and p_{x0} and p_{y0} are the initial transverse momentums, and $\beta_{o\perp} = |e|\hbar A_w/(\gamma m_o c^2)$.

The particle motion in the y-direction is due to the finite z-component of the wiggler field,

$$\frac{dp_y}{dt} = \frac{|e|\hbar}{c} v_z B_z. \quad (4)$$

We will assume that the fast oscillatory terms are unimportant. Replacing v_z by c in the appropriate places, we find that

$$\frac{d^2 \hat{y}}{dz^2} + \frac{1}{4} \beta_{o\perp}^2(z) k_w(z) \sinh(2k_w(z) \hat{y}) = 0. \quad (5)$$

Taking $k_w(z) \hat{y} \ll 1$, this equation can be integrated to give

$$\hat{y} \simeq y_\beta \left(\frac{k_\beta(0)}{k_\beta(z)} \right)^{1/2} \cos\left(\int_0^z k_\beta(z') dz' + \phi_\beta \right), \quad (6)$$

where $k_\beta = \beta_{o\perp} k_w / \sqrt{2}$, $y_\beta = (\bar{p}_{y0}^2 + y_o^2)^{1/2}$, $\bar{p}_{y0} = p_{y0} / k_\beta(0) \gamma m_o c^2$, and $\phi_\beta = \cos^{-1}(y_o / y_\beta)$.

RADIATION FIELD

The radiation field can be written in terms of Gaussian resonator modes. For the purpose of illustrating this resonance, only the TEM_{00} mode will be considered, i.e.,

$$\mathbf{A}_R(x, y, z, t) \simeq -A_{00}(z) G_{00}(x, y, z) \exp(i(kz - \omega t)) \hat{\mathbf{e}}_x + c.c., \quad (7)$$

where $A_{00}(z) = |A_{00}(z)| \exp(i\phi_{00}(z))$ is the slowly varying self-consistent complex amplitude,

$$G_{00}(x, y, z) = g_{00} \exp(i\theta_{00}), \quad (8)$$

$$g_{00}(x, y, z) = \frac{w_o}{w(z)} \exp\left(\frac{-(x^2 + y^2)}{w^2(z)} \right),$$

$$\theta_{00}(x, y, z) = -\tan^{-1} \zeta + \left(\frac{x^2 + y^2}{w^2(z)} \right) \zeta,$$

$\zeta = (z - L_c) / z_o$ is the normalized axial distance, $w(z) = w_o(1 + \zeta^2)^{1/2}$, ω and $k = \omega/c$ are the frequency and wavenumber of the radiation, w_o is the waist of the resonator mode, $z_o = w_o^2 k / 2$ is the Rayleigh length, and L_c is the axial location of the minimum waist.

Gaussian decomposition of the radiation field has been outlined in several different contexts [2,17]. This formulation differs from Ref. [17] in that we include betatron oscillations and finite beam emittance.

The slowly varying complex amplitude of the radiation field is governed by

$$\frac{da_{00}(z)}{dz} = i\alpha F a_w(z) e^{i\phi_{00}(z)} \left\langle \frac{\cosh(k_w(z)\tilde{y}) g_{00}(\tilde{x}, \tilde{y}, z)}{\tilde{\gamma}} e^{-i\psi} \right\rangle, \quad (9)$$

where

$$\alpha = \frac{1}{2k} \frac{\omega_b^2}{c^2} \frac{v_{zo}}{c},$$

$$\psi(x_o, y_o, p_{xo}, p_{yo}, \psi_o, z) = \int_0^z (k + k_w(z') - \omega/\tilde{v}_z) dz' + \theta_{00}(\tilde{x}, \tilde{y}, z) + \phi_{00}(z) + \psi_o$$

is the phase of the electron in the ponderomotive potential well, ψ_o is the initial phase at $z = 0$,

$$\langle (...) \rangle = \int_0^{2\pi} \frac{d\psi_o}{2\pi} \int dx_o \int dy_o \int dp_{xo} \int dp_{yo} (...) W(x_o, y_o, p_{xo}, p_{yo}, \psi_o)$$

is the average over all electrons in the transverse direction and one period of the ponderomotive potential wave, W is the initial electron distribution function such that $\langle (1) \rangle = 1$, $\omega_b = (4\pi|e|^2 n_o/m_o)^{1/2}$ is the plasma frequency, n_o is the peak electron density, $F = \sigma_b/\pi w_o^2$ is the 1-dimensional filling factor, σ_b is the area of the electron beam, $a_w = |e|A_w/m_o c^2$ and $a_{00} = |e|A_{00}/m_o c^2$.

EQUATION OF PHASE

The equation of phase for the electron entering the wiggler with the initial condition $(x_o, y_o, p_{xo}, p_{yo}, \psi_o)$ in the ponderomotive potential well can be written in the form

$$\frac{\partial^2 \psi}{\partial z^2} = -K_{so}^2 \cosh(k_w(z)\tilde{y}) e^{\left(-\frac{\tilde{x}^2 + \tilde{y}^2}{w^2(z)}\right)} [\sin \psi - \sin \psi_R], \quad (10)$$

where

$$K_{so}(z) = \left(\frac{1}{\gamma^2} \frac{w_o}{w(z)} k_w k a_w(z) |a_{00}(z)| \right)^{1/2}$$

is the synchrotron wavenumber of the electrons traveling exactly along the z -axis. The instantaneous synchrotron wavenumber for the off-axis electrons is

$$K_s(x_o, y_o, p_{xo}, p_{yo}, z) = K_{so}(z) \left(\cosh(k_w(z)\tilde{y}) \exp\left(-\frac{\tilde{x}^2 + \tilde{y}^2}{w^2(z)}\right) \right)^{1/2}.$$

The resonant phase ψ_R is determined by the expression

$$\begin{aligned} \sin \psi_R(x_o, y_o, p_{xo}, p_{yo}, z) = & \sin \psi_{Ro} + \Delta(\tilde{x}, \tilde{y}, z) \sin \psi_{Ro} + \frac{1}{K_o^2} \frac{d^2 \theta_{00}}{dz^2} \\ & + \frac{k}{8\gamma^2 K_o^2} y_\beta^2 \frac{k_\beta(0)}{k_\beta(z)} (1 + \cos \Phi) \frac{d[a_w^2(z)k_w^2(z)]}{dz}, \end{aligned} \quad (11)$$

where

$$\Phi(y_o, p_{yo}, z) = 2 \int_0^z k_\beta(z') dz' + 2\phi_\beta,$$

$$\sin \psi_{Ro}(z) = T(z)/K_{so}^2(z)$$

is the resonant phase of electrons traveling exactly along the z-axis, and

$$T(z) = \left[\frac{dk_w}{dz} - \frac{k}{4\gamma^2} \frac{da_w^2}{dz} + \frac{\omega}{c} \frac{1+a_w^2}{\gamma^3} \frac{|e|}{m_o c^2} \frac{\partial \phi_{DC}}{\partial z} \right]$$

is the degree of taper for the efficiency enhancement schemes, which can be achieved by increasing the wiggler wavenumber, decreasing the amplitude of the wiggler vector potential, or by applying a DC accelerating electric field. For efficiency enhancement, the resonant phase has to be positive and less than unity.

In the betatron-synchrotron instability the resonant phase is forced to oscillate at the wavenumber $2k_\beta$. If the wavenumber of the electrons about the separatrix is $\simeq 2k_\beta$, then an instability can occur. As electrons execute betatron oscillations, the electrons experience a varying radiation amplitude and phase, which are contained in the second and the third terms on the right-hand side of Eq. (11). The tapering of the wiggler B_w can also result in an oscillatory driving term, i.e., the fourth term on the right-hand side of Eq. (11). This process is discussed in detail in Ref. [5]. If the oscillation frequency of the resonant phase matches the frequency of the electrons going around the resonant phase, the synchrotron frequency, then the phase of the electrons in the ponderomotive potential well will oscillate with increasing amplitude, and eventually the electrons become detrapped.

The radiation amplitude variation felt by the electrons not only results in a spatially dependent bucket size, but also in forced oscillations of the resonant phase, the second term of Eq. (11), where

$$\Delta(\tilde{x}, \tilde{y}, z) = 1 - \frac{1}{\cosh(k_w(z)\tilde{y})} \exp\left(\frac{\tilde{x}^2 + \tilde{y}^2}{w^2(z)}\right).$$

Since \tilde{y}^2 and $\cosh(k_w(z)\tilde{y})$ are both periodic functions of Φ , the coefficient of the second term in Eq. (11) is also a periodic function of Φ .

The variation in phase felt by the electrons, due to the betatron oscillations, contributes the third term on the right-hand side of Eq. (11). Substituting (6) into (8), we obtain

$$\frac{d^2\theta_{00}(x_o, y_o, p_{xo}, p_{yo}, z)}{dz^2} = f_o + f_c \cos \Phi + f_s \sin \Phi, \quad (12)$$

$$f_c(y_o, p_{yo}, z) = \frac{y_\beta^2}{w^2(z)} \frac{k_\beta(0)}{k_\beta(z)} \left[\frac{\zeta^2 - 3}{z_o^2(1 + \zeta^2)^2} - 2k_\beta^2(z) \right] \zeta,$$

$$f_s(y_o, p_{yo}, z) = -2 \frac{y_\beta^2}{w^2(z)} \frac{k_\beta(z)}{z_o} \left[\frac{1 - \zeta^2}{1 + \zeta^2} \right],$$

and

$$\begin{aligned} f_o(x_o, y_o, p_{xo}, p_{yo}, z) = & \frac{1}{z_o^2} \frac{2\zeta}{(1 + \zeta^2)^2} \left[\frac{\zeta^2 - 3}{2w^2(z)} \left(\tilde{x}^2 + \frac{k_\beta(0)}{k_\beta(z)} \frac{y_\beta^2}{2} \right) + 1 \right] \\ & + \frac{2}{w^2(z)} \left[\frac{2\beta_{xo}\tilde{x}}{z_o} \frac{1 - \zeta^2}{1 + \zeta^2} + \beta_{xo}^2 \zeta \right]. \end{aligned}$$

We note that each term on the right-hand side of Eq. (12) is highly dependent on the initial conditions as well as the axial position z . The phase variation term $(1/K_s^2)d^2\theta_{00}/dz^2$ does not have a spatial variation equal to $2k_\beta$, because the coefficients K_s , f_s , f_c , and f_o are functions of z . Hence, the effectiveness of the phase variation term in driving the betatron-synchrotron instability is reduced.

The strongest effect of the resonance on the gain is not at $K_{so} = 2k_\beta(0)$, because the synchrotron wavelength associated with electrons undergoing betatron oscillation is longer than that associated with electrons traveling exactly on axis. This is a consequence of

the larger radiation field on axis. In addition, the synchrotron wavelength of the electrons initially close to the resonant phase ψ_R is $2\pi/K_s$. The synchrotron wavelength of the electrons, that were initially trapped further away from the resonant phase, is longer than $2\pi/K_s$. Hence, the more accurate resonant condition is

$$6k_\beta > K_{so} > 2k_\beta. \quad (13)$$

NUMERICAL EXAMPLES

We present numerical results illustrating various properties of this instability. The linearly polarized wiggler amplitude is $B_w(0) = 3$ kG, and the wavelength is $\ell_w(0) = 2.73$ cm. The wiggler length is $L_w = 150$ cm, the minimum waist is located at $z = 75$ cm, and the electron beam energy is 20.8 MeV. The electron density on axis is $n_o = 2.5 \times 10^{11} \text{ cm}^{-3}$, which corresponds to a plasma frequency ω_b of $2.8 \times 10^{10} \text{ sec}^{-1}$. Radiation wavelength is $10 \mu\text{m}$, with a Rayleigh length $z_o = 62.5$ cm and spot size $w_o = 0.14$ cm. The betatron wavenumber is $k_\beta = 0.03 \text{ cm}^{-1}$ and the betatron wavelength is $L_\beta = 2\pi/k_\beta = 210$ cm.

A Gaussian electron distribution function is chosen:

$$W = C \exp\left(-\frac{x_o^2}{r_{eb}^2}\right) \exp\left(-\frac{y_o^2 + p_{yo}^2}{r_{eb}^2}\right),$$

where C is the normalization constant, and $p_{zo} \equiv 0$.

Here we present results where k_w is tapered and a_w is held constant. The taper of k_w is linear, i.e.,

$$k_w(z) = k_w(0)(1 + \delta z),$$

where $\delta = 1/L_c$, and L_c is the length the wavenumber increases by $k_w(0)$. For a linear variation of k_w , $\sin \psi_{Ro}$ is not a constant. The constant δ is chosen such that $\sin \psi_{Ro}(z = L_w) = 0.4$. The parameters that will be varied are the betatron-synchrotron wavenumber mismatch ratio

$$\rho = \frac{K_{so}(z = L_c)}{2k_\beta(0)},$$

and the radius of the electron beam r_{eb} .

Figures 1-6 show the results obtained with $\rho = 2.0$ and $r_{eb} = w_o$. For these parameters, the second term on the right-hand side of Eq. (11) is the largest oscillatory driving term. For electrons with the same initial conditions (x_o, y_o, p_{yo}) but $-\pi \leq \psi_o \leq \pi$, Figs. 1, 3, 5 are plots of ψ versus $\partial\psi/\partial z$ and Figs. 2, 4, 6 are plots of ψ versus z . Each curve represents the history of an electron in the phase space from $z = 0$ to $z = L_w$.

Figures 1 and 2 are plots of phase for electrons traveling exactly down the axis, i.e., $x_o = 0$, $y_o = 0$, and $p_{yo} = 0$. Electrons that are initially trapped remain trapped.

Figures 3 and 4 are plots of phase for electrons with initial conditions $x_o = w_o$, $y_o = 0$, and $p_{yo} = 0$. These electrons do not execute betatron oscillations. Since they are on the edge of the radiation beam, the bucket size is reduced, and only 40% of the electrons are initially trapped, these trapped electrons remain trapped to the end of the wiggler.

Figures 5 and 6 are phase plots for electrons with initial conditions $x_o = 0$, $y_o = w_o$, and $p_{yo} = 0$. If these electrons did not undergo betatron oscillations, their phase space diagrams would be identical to those in Figs. 3 and 4. We notice that 25% of the electrons become detrapped at $z \simeq 100 \text{ cm} \simeq \pi/k_\beta(0)$. Only 20% of the electrons remain trapped at the end of the wiggler.

The numerical results confirm that the synchrotron wavelengths associated with Figs. 3-6 are much longer than those of Figs. 1-2, because the radiation amplitude felt by the electrons on axis is larger than the the average radiation field felt by the electrons undergoing betatron oscillations.

Figure 7 is a plot of normalized relative amplitude gain,

$$G_n = \frac{g/r_{eb}^2}{g/r_{eb}^2|_{r_{eb} \rightarrow 0}}$$

versus r_{eb}/w_o for $\rho = 1.4$, $\rho = 2.0$, and $\rho = 2.9$. The solid curves are the results with betatron oscillations, and the dashed curves are the results without betatron oscillations. The results are almost identical for $r_{eb}/w_o < 0.8$. There is a small reduction of the gain when $r_{eb}/w_o = 1$ for $\rho = 2.0$ and $\rho = 1.4$. The reduction is small because the distribution function associated with the electrons that take part in the betatron-synchrotron instability is small.

In conclusion, we identified three different sources responsible for the betatron- synchrotron instability: the radiation phase front curvature, the transverse radiation amplitude variation in an FEL with efficiency enhancement schemes, and the tapering of the magnetic wiggler field amplitude. For the parameters considered in this paper, the radiation amplitude variation is found to be the largest driving term. For short wigglers of this example, i.e., $L_w \simeq 1.5\pi/k_\beta$, and $r_{eb}/w_o \leq 0.8$, the effect of betatron-synchrotron instability on the gain is negligible.

Acknowledgment

This work is sponsored by DARPA under Contract 3817.

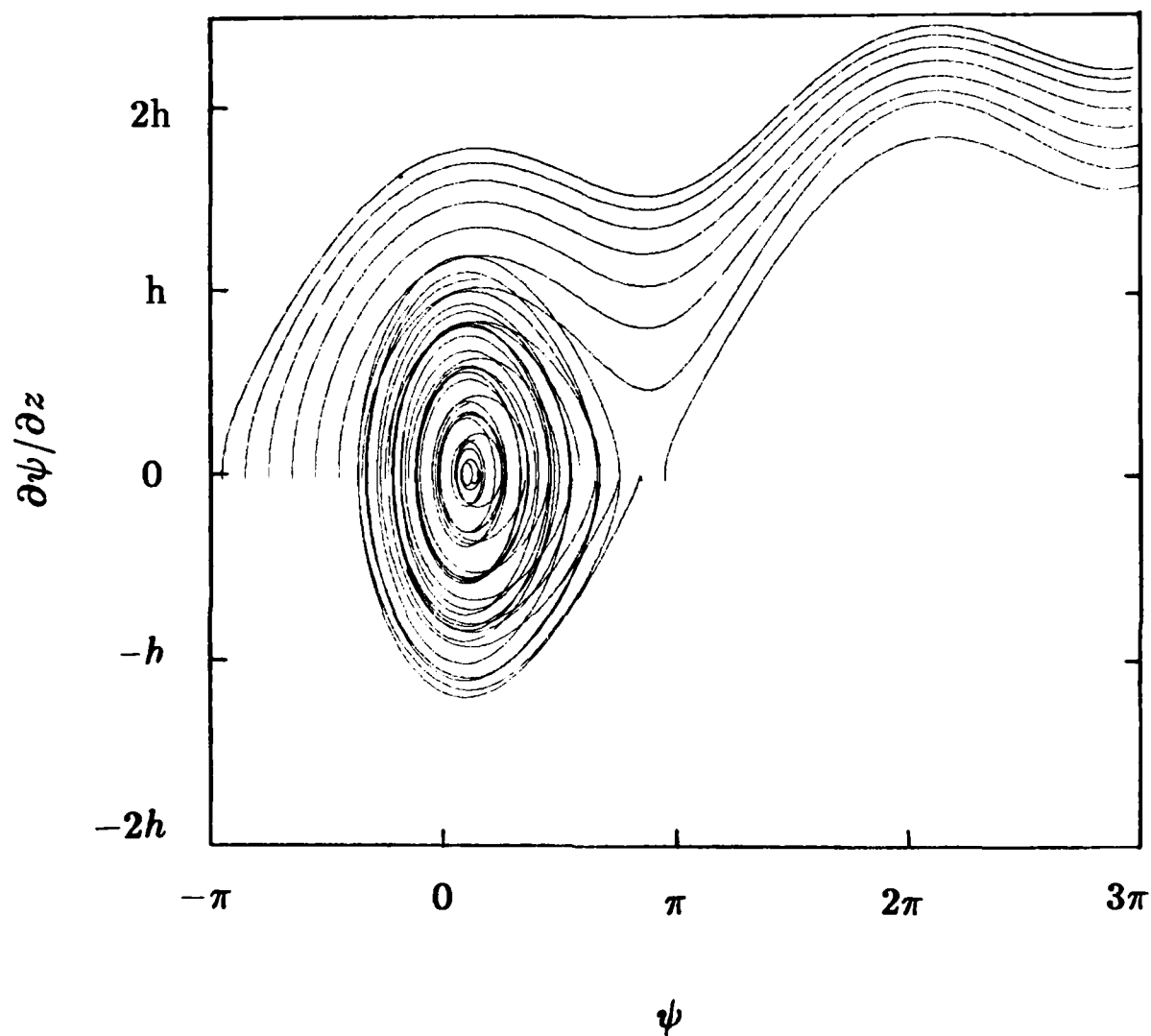


Fig. 1. Plot of ψ versus $\partial\psi/\partial z$ for electrons with initial condition $x_o = 0$, $y_o = 0$, and $p_{yo} = 0$.

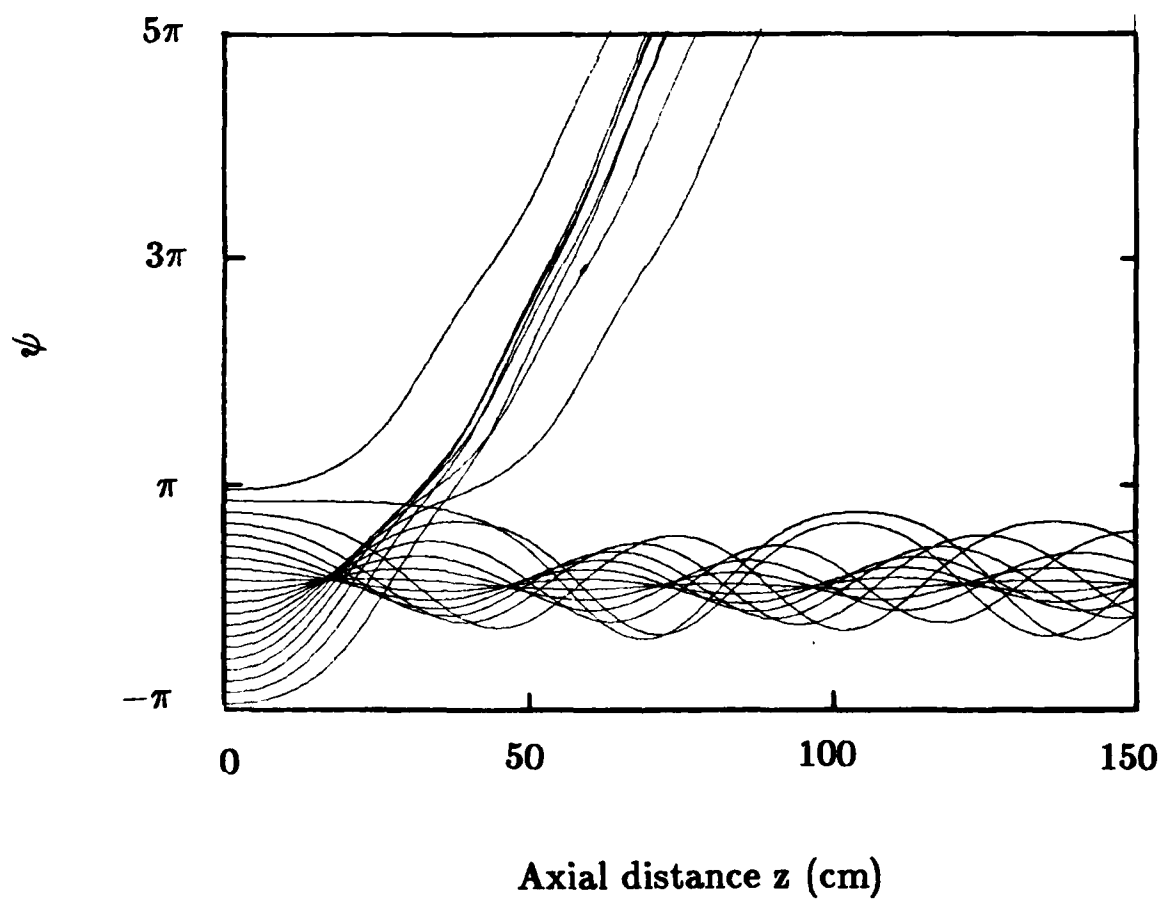


Fig. 2. Plot of ψ versus z for electrons with initial condition $x_o = 0$, $y_o = 0$, and $p_{yo} = 0$.

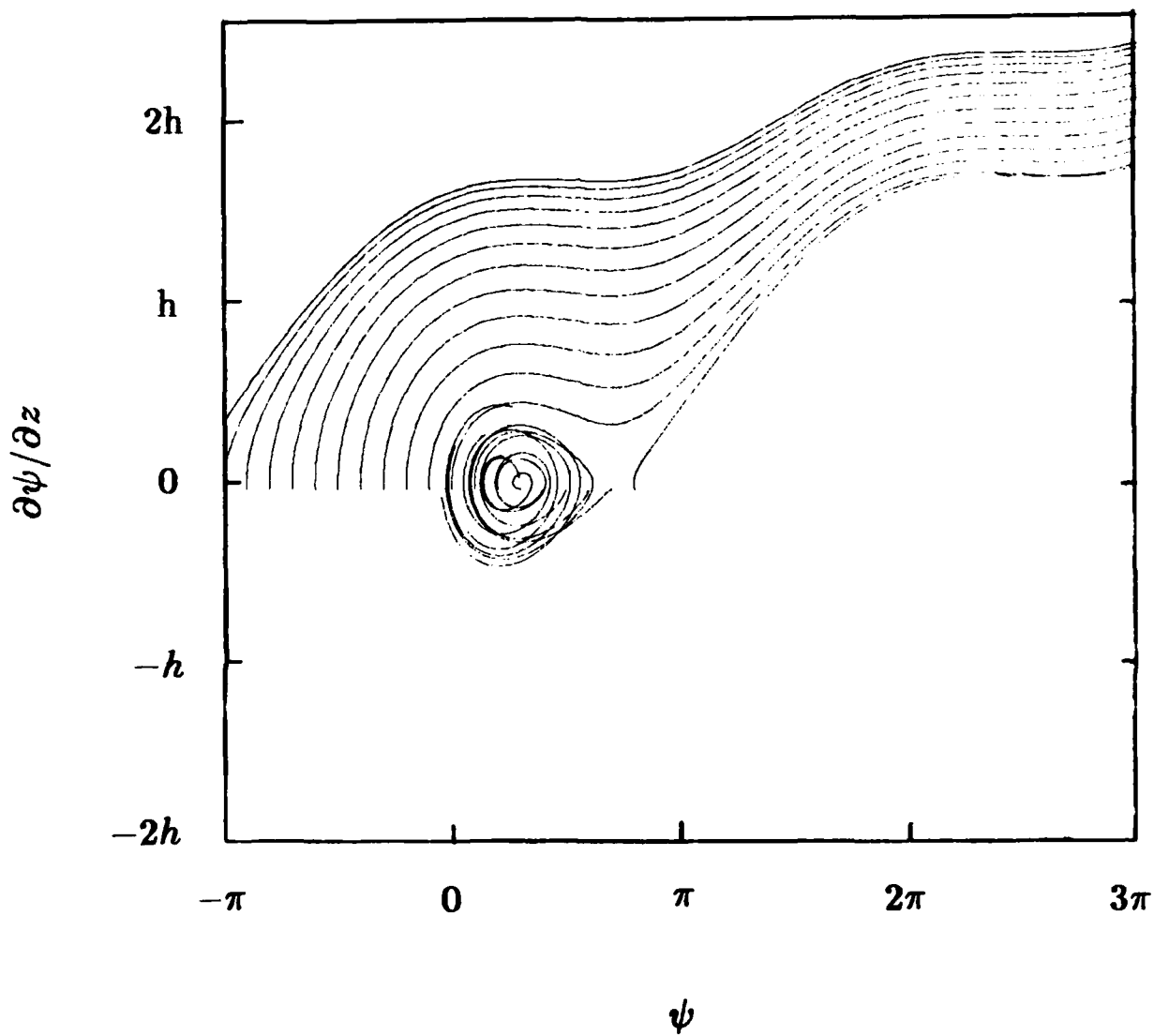


Fig. 3. Plot of ψ versus $\partial\psi/\partial z$ for electrons with initial condition $x_o = w_o$, $y_o = 0$, and $p_{y_o} = 0$.

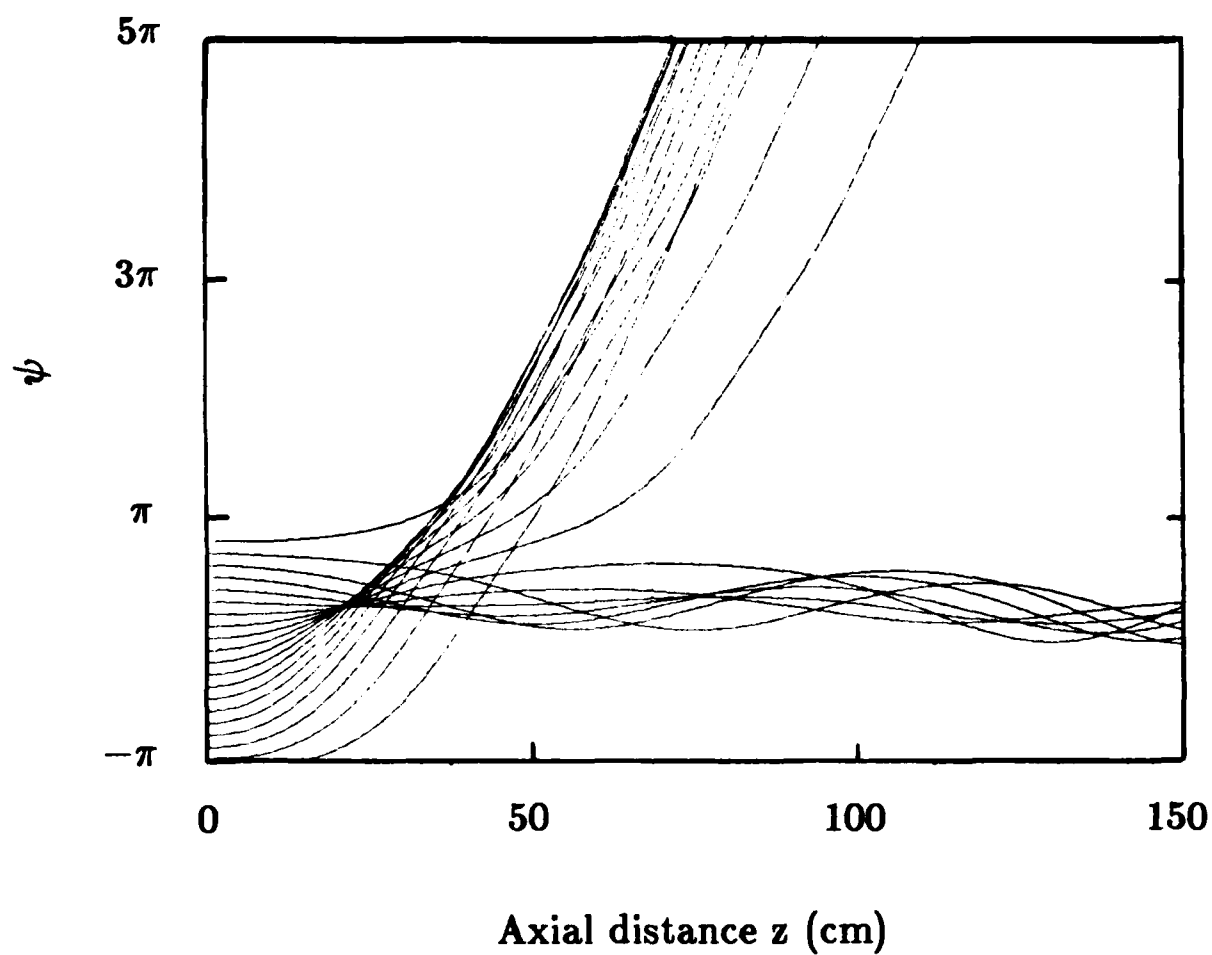


Fig. 4. Plot of ψ versus z for electrons with initial condition $x_o = w_o$, $y_o = 0$, and $p_{y_o} = 0$.

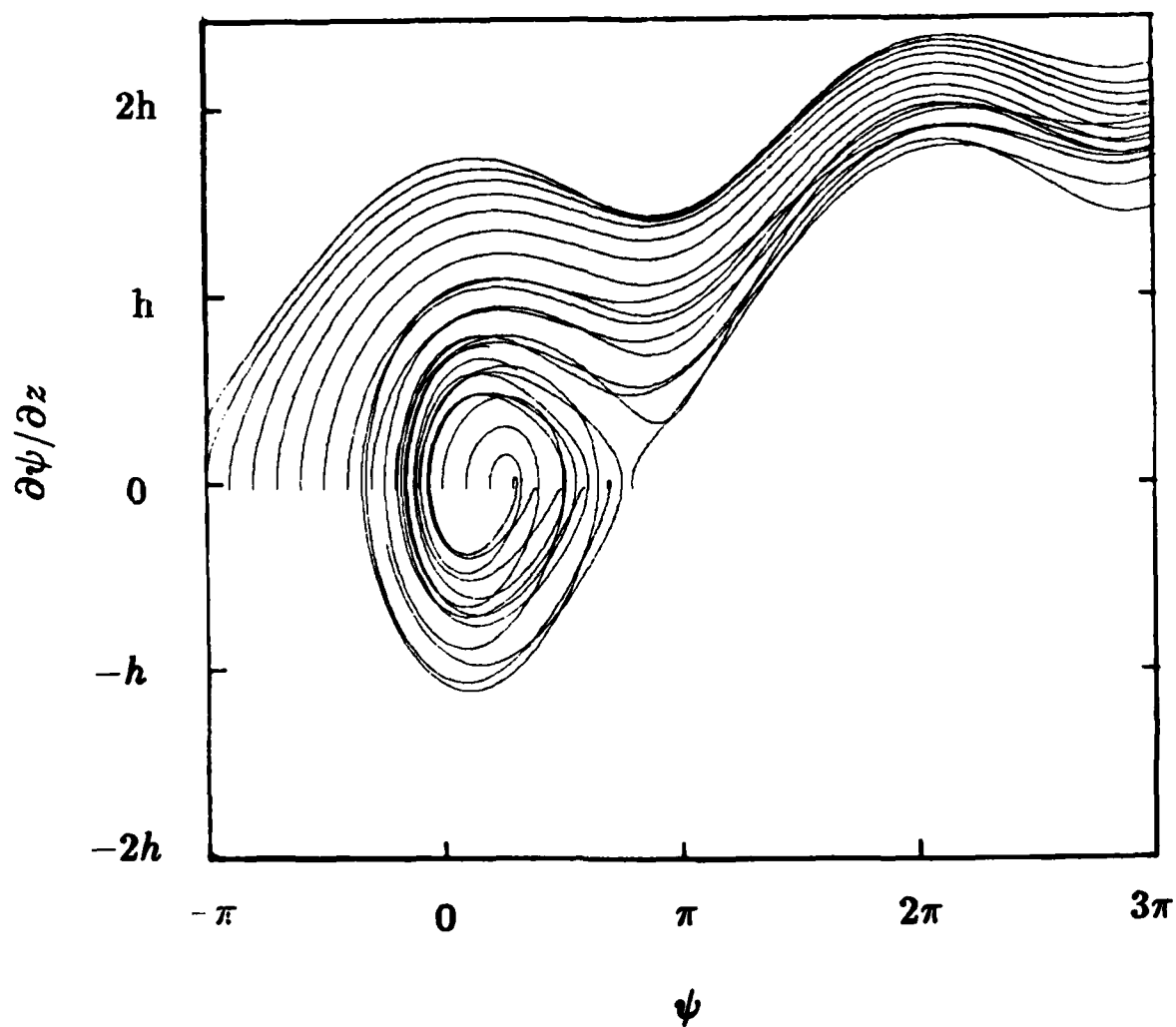


Fig. 5. Plot of ψ versus $\partial\psi/\partial z$ for electrons with initial condition $x_o = 0$, $y_o = w_o$, and $p_{yo} = 0$.

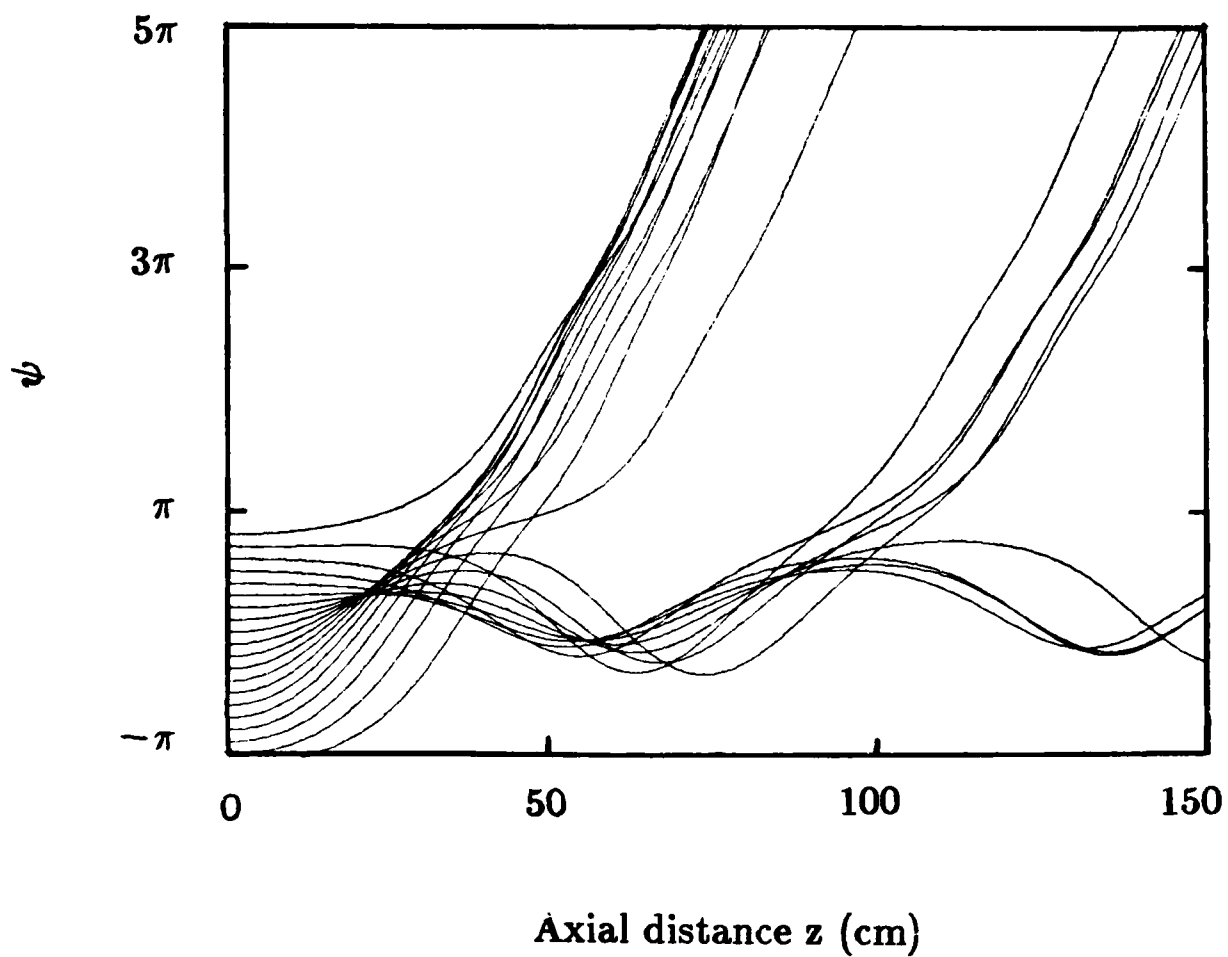


Fig. 6. Plot of ψ versus z for electrons with initial condition $x_o = 0$, $y_o = w_o$, and $p_{y_o} = 0$.

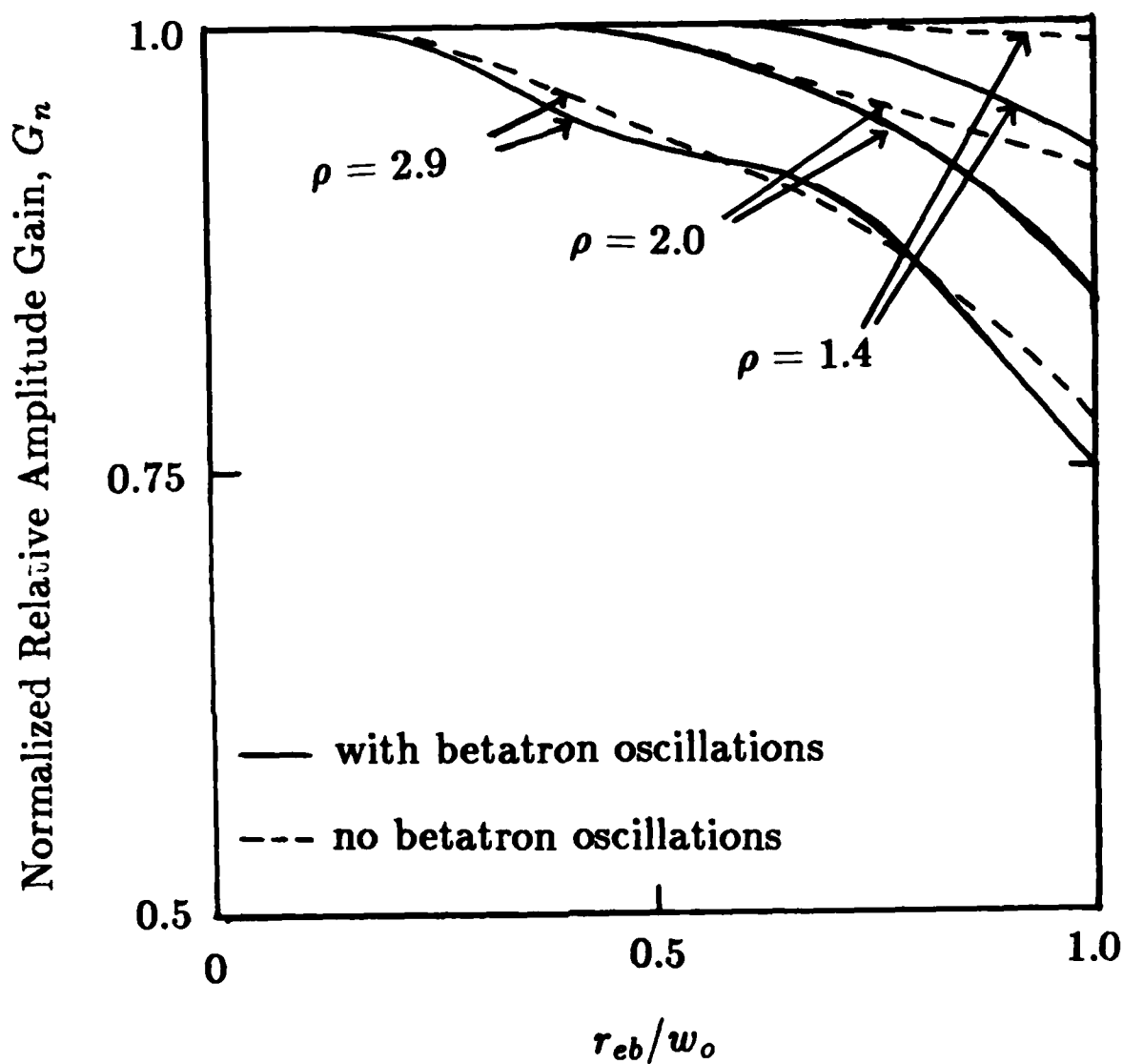


Fig. 7. Plot of normalized relative amplitude gain versus r_{eb}/w_o for betatron-synchrotron wavenumber mismatch ratio $\rho = 1.4$, $\rho = 2.0$, and $\rho = 2.9$.

References

- [1] M. N. Rosenbluth, "Two-Dimensional Effects in FEL's", paper No. I-ARA-83-U-45 (ARA-488), Austin Research Asso., TX (1983).
- [2] C.-M. Tang and P. Sprangle, "Semi-Analytical Formulation of the Two-Dimensional Pulse Propagation in the Free Electron Laser Oscillator", Free-Electron Generators of Coherent Radiation, SPIE Proc. 453, (ed. by C. A. Brau, S. F. Jacobs and M. O. Scully), Bellingham, WA, p.11 (1983).
- [3] C.-M. Tang, "Particle Dynamics Associated with a Free Electron Laser", to be published in the Proc. of Lasers '83, held at San Francisco, CA, Dec 12-16, 1983.
- [4] W. M. Fawley, D. Prosnitz and E. T. Scharlemann, accepted for publication in Phys. Rev. A.
- [5] P. Sprangle and C.-M. Tang, "Betatron-Synchrotron Detrapping in a Tapered Wiggler Free Electron Laser", NRL Memo. Report 5445.
- [6] T. I. Smith and J. M. J. Madey, Appl. Phys. **B27**, 195 (1982).
- [7] P. Diament, Phys. Rev. **A23**, 2537 (1971).
- [8] V. K. Neil, "Emittance of Transport of Electron Beam in a Free Electron Laser", SRI Tech. Report JSR-79-10, SRI International (1979). AD-A081-064
- [9] C.-M. Tang, Proc. of the Intl. Conf. on Lasers '82, 164 (1983).
- [10] P. Sprangle and C.-M. Tang, Appl. Phys. Lett. **39**, 677 (1981).
- [11] C.-M. Tang and P. Sprangle, Free-Electron Generators of Coherent Radiation, [Phys. of Quantum Electronics, Vol. 8], ed. by Jacobs, Moore, Pilloff. Sargent, Scully and Spitzer, Addison- Wesley Publ. Co., Reading, MA, p.627 (1982).
- [12] A. Gover, H. Freund, V. L. Granatstein, J. H. McAdoo and C.-M. Tang, "Basic Design Considerations for Free Electron Laser Driven by Electron Beams from RF Accelerators", Infrared and Millimeter Waves, Vol. 12, ed. K. J. Button.
- [13] N. M. Kroll, P. L. Morton and M. N. Rosenbluth, IEEE J. of Quantum Elec. **QE-17**, 1436 (1981).
- [14] P. Sprangle, C.-M. Tang and W. M. Manheimer, Phys. Rev. Lett. **43**, 1932 (1979).
- [15] P. Sprangle, C.-M. Tang and W. M. Manheimer, Phys. Rev. **A21**, 302 (1980).
- [16] C.-M. Tang and P. Sprangle, J. Applied Phys., **52**, 3148 (1981).

[17] P. Elleaume and D. A. G. Deacon, Appl. Phys. B33, 9 (1984).

END

FILMED

3-85

DTIC